Chapter 2

Porous Titanium by Powder Metallurgy for Biomedical Application: Characterization, Cell Citotoxity and *in vivo* Tests of Osseointegration

Luana Marotta Reis de Vasconcellos, Yasmin Rodarte Carvalho, Renata Falchete do Prado, Luis Gustavo Oliveira de Vasconcellos, Mário Lima de Alencastro Graça and Carlos Alberto Alves Cairo

Additional information is available at the end of the chapter

http://dx.doi.org/10.5772/47816

1. Introduction

Surgical implants are used to replace lost body structures and due to the increased life expectancy of the world population, they have become one of the most promising fields for improving the quality of life of these individuals [1]. The biological process of osseointegration or calcified bone matrix apposition on the surface of a synthetic implanted material constitutes one of the most important discoveries of clinical practice of the 20th century. However, there are areas of knowledge that are not fully understood, particularly involving the biochemistry of bone formation, cellular response and the regulatory mechanisms of osteogenesis and bone resorption. Currently, implant dentistry focuses on studies that address and enable more rapid osseointegration of implants for orthopedic and dental use, in an attempt to reduce or even eliminate the period of bone healing free from functional load [2]. Among the various lines of research oriented toward this purpose, the topographical characteristics of the implant surface at the bone-implant interface are considered relevant due to the strong influence on the quality of osseointegration achieved [3-8], together with the characteristics of the biomaterial from which the implant is produced [3,9-11].

Metals are the most commonly used biocompatible materials in commercial manufacturing of surgical implants, while titanium (Ti) and its alloys are the most commonly used metals in the field of biomedicine [3-10,12], due to their excellent physical and chemical properties. Titanium has proven biocompatibility and an extraordinary combination of properties, since it exhibits high tensile strength (200-700 MPa), low specific weight (density = 4.5 g/cm^3 at

25°C), a high melting point (1688°C), a modulus of elasticity compatible with calcified body tissues (110 GPa), Vickers hardness between 80 and 105 that varies depending on the purity of Ti, thermal conductivity of 0.2 J/cm.K and thermal expansion of $9{:}6x10^{-7}$ K^{-1} [13].

The main limitation of Ti is its chemical reactivity with other materials, at high temperatures. However, at room temperature, when in contact with air, Ti loses this reactivity, becoming extremely inactive. This phenomenon, denominated passive, results in the formation of a very thin oxide film that is highly adherent to the metal surface, which serves as a protective barrier to further corrosion [13]. This thin layer is formed mainly by titanium dioxide (TiO_2), which appears amorphous, insoluble and very stable and can form again when removed mechanically. Besides this limitation, Ti exhibits another drawback to its use in clinical practice, orthopedics and dentistry, which is the difference between the modulus of elasticity of the metallic implant of Ti (110GPa) and the modulus of elasticity of bone tissue (10-30GPa) [14]. However, this drawback can be controlled with the fabrication of pores in the structure of Ti implants [9,15] or with new Ti allows of low modulus of elasticity [16].

Regardless of the surface topography of Ti, the bioactivity of this surface is not sufficient to induce the growth of bone tissue in a short period. Several studies have demonstrated greater osteoconductivity of Ti implants that were subjected to thermal and chemical treatments. These treatments, called biomimetics, are specific processes capable of forming in vitro on the implant surface by ion precipitation using calcium phosphates, such as hydroxyapatite ($Ca_5(PO_4)_3(OH)$) [17-21].

Biomimetic methods for HA coating on Ti are based on the nucleation and growth of calcium phosphate in simulated body fluid following preheat treatment [17]. This treatment aims to produce an apatite layer on the surface of Ti implants, increasing their osteoconductivity, consequently favoring osseointegration. Bioactive coating on the porous surface is an attractive method to improve the quality of the bone-implant interface, particularly in the initial stages of healing [21].

Implant topography and surface chemical structure are two aspects considered important for osseointegration, since topography is related to fibrin clot retention and osteoprogenitor cell migration, while the chemical structure influences the surface adsorption of proteins that promote adhesion and the activation of osteoprogenitor cells [20].

Porosity can be defined as the percentage of void spaces in a solid. The osseointegration obtained with porous Ti is achieved by bone growth into the pores, called "bone ingrowth", which improves micromechanical interlocking, the interlacing of bone tissue within the implant, preventing mobility.

Numerous studies have shown that implant porosity promotes positive results in bone neoformation in vivo [4,5,8-10,22,23], since it increases the contact area between the biomaterials and bone tissue [4,22], resulting in improved implant stability over time, as well as accelerating the process of osseointegration [24]. Concomitantly, various studies have shown that the implant surface can alter the metabolism and phenotypic expression of osteoblastic cells [22,23,25].

A porous surface with interconnected pores results in significant improvement in the rate of bone formation and in better fixation of the implant to the bone [20,21]. The porous structure must be produced with high porosity to provide sufficient space for cell adhesion and subsequent formation of new bone that permits the transport of body fluids and the proliferation of new vasculature, while providing adequate mechanical properties to withstand stresses during implantation and use [4-8,12,22]. However, although increased porosity and pore size favors new bone growth, this increase can diminish the mechanical properties of the implant [6-8,26].

Xue et al. [27] showed that effects like increased cell attachment, cell differentiation, alkaline phosphatase expression occur when using porous Ti samples with pores larger than 200μm. Osteoblasts respond differently depending on the pore size. In pores smaller than 100μm, the cells spread directly on top of the pore by filopodia, while in pores larger than 200μm, osteoblasts do not spread over the pore, growth within the pores is observed. In an extensive review, Karageorgiou and Kaplan [28] considered that the minimum pore size should be 100μm due to cell size and the characteristics of cell migration and transport. However, pores of 300μm are considered ideal, since they facilitate the formation of capillaries. It is also possible to correlate this data with the size of Haversian channels of approximately 100-200μm in diameter. Small pores could favor hypoxia, which can result in the formation of osteocartilaginous tissue, while large richly vascularized pores permit direct osteogenesis. The authors conclude by recommending the development of technologies that can produce a gradient of pore sizes, resulting in an improved bone-implant interface.

Osteoblasts in culture were capable of covering distances of 600μm in diameter to populate a channel in a Ti sample, forming cell bridges [24]. In channels 300μm in diameter, a single cell was capable of creating extensions side to side by filopodia. The capacity to quickly cellularize a channel is inversely proportional to cell differentiation. Once attached to the wall of the channel a cells begins its differentiation, increasing the expression of molecules such as osteocalcin, osteopontin, fibronectin, collagen I and III. From a morphological point of view, in this study, a diameter of 600μm was favorable to cell response. Lamellar bone formation occurs within pores of 100, 200 and 300μm. However, it has been reported that for implants with pores of 100μm, the bone formation rate was lower and for 300μm, it was initially slower than for a pore size of 200μm. Thus, the optimal size for surface structuration of Ti implants was 200μm [29].

High porosity facilitates the transport of body fluids, benefits the spread of cells into the implant and promotes the proliferation of bone tissue, since it increases the contact area [4,5] however, equilibrium between the rate of porosity and mechanical properties of the material should be maintained.

Some researchers have reported that the percentage of pores suitable for Ti samples is between 25 and 66% [30,31]. Takemoto et al. [32] suggested that porous Ti with 40% porosity could be an alternative for clinical use. However, samples of 5 and 80% porosity have also shown bone formation [33]. Increased porosity permits the growth of tissue into the pores

and, subsequently, mineralization [30]; however, maintaining the mechanical properties of the implant is fundamental. The ideal microtopography for commercial porous implants remains undetermined.

Currently, researchers are attempting to develop implants based on a multifactorial vision, since it is necessary to consider the mechanical properties of the biomaterial, such as corrosion resistance, passivity levels and bone adherence potential, together with mechanical properties that include the deformation behavior of the porous material and its relation to the bone in which it is implanted, in order to withstand the conditions of daily loading. Finally, parameters involving diameter, shape and the distribution of pores that will enhance the fatigue strength and proliferation of bone tissue should also be considered [34].

In order to promote optimal tissue integration with the surgical implant, interactions at the biomaterial-host tissue interface should be optimized. Thus, researchers are strongly committed to modify the surface of Ti implants to improve and accelerate the cellular response [35], since cells interact with the outermost layer of the implant, thus conferring an important role to the implant surface in the initial response of the patient [36]. These interactions occur at the cellular level and, therefore, it is necessary to develop new biomaterials with controlled surface characteristics that are able to directly influence cells.

2. Biomimetic treatment

Surface modifications of Ti that have been described in the literature have greatly improved surface contact at the bone-implant interface and reduced repair time. This result is attributed to increased osteoblastic activity on the surface of the implants [37]. However the cellular mechanisms have not been fully elucidated [38].

Studies have reported that topography can determine the adsorption of biomolecules and their orientation on the surface of the implant, immediately following installation of the same in the surgical cavity. Furthermore, it may influence the early formation of fibrin clots, platelet activation and the production of growth factors related to bone tissue, thereby interfering directly in cell recruitment, adhesion, proliferation and differentiation [24]. Evidence suggests that the mechanism by which the topography of Ti influences the differentiation of osteoblasts is related to the pathways of phospholipase A2, protein kinase A and integrin. Cells growing on roughened Ti surfaces present increased expression of TGF-β1 and interleukin Iβ and a prostaglandin-mediated response, which leads to decreased proliferation and favors cell differentiation with an increase in alkaline phosphatase activity and increased expression of molecules, such as osteocalcin [39,40].

Hydroxyapatite corresponds to the main mineral component of human bone tissue. However, its poor mechanical properties limit its practical applications as implants subjected to loading. More recently, implants based on Ti coated with bioinert apatite or hydroxyapatite have attracted a lot of attention because these coatings result in a biomaterial that combines the advantageous mechanical properties of Ti with the biological affinity of bone to hydroxyapatite [41].

Therefore calcium phosphate coatings have been widely investigated due to their chemical similarity with the bone mineral portion. Several chemical and physical techniques have been developed to deposit thin coatings on metals in order to form a bioactive surface layer capable of chemically binding to bone that also accelerates the process of bone apposition, particularly during the initial period of healing.

Among the methods of applying calcium phosphate, thermal blasting by plasma spraying has been the most widely used technique commercially. This technique consists of pulverizing ceramic particles on the implant surface from a plasma spray at high temperature. Although this provides a highly osteoconductive surface [42], researchers have reported that this technique does not permit precise control of the chemical composition and crystal structure of calcium phosphate formed on the metal [43], which could provoke a mechanically and chemically unstable and weak bond between the metal substrate and bone. It is difficult to achieve uniform thickness of the deposited layer and difficult to use on implants with complex geometries [44].

In 1996, Kokubo et al. published studies showing a chemical treatment method for Ti that promotes the deposition of apatite on its surface, in order to induce bioactivity for use in endosseous implants. Heating in alkali was performed to form sodium titanate on the surface, followed by immersing the specimens in a simulated body fluid (liquid ionic conditions simulating blood plasma), resulting in the formation of an apatite layer on the samples. The term biomimetic treatment is attributed to this type of process. According to the authors, bioactive Ti and its alloys could be used as bone substitute materials, even in conditions requiring mechanical loads. According to Chen et al. [41], Ti implants coated with apatite or hydroxyapatite combine the advantages of the biomechanical strength of the metal with the biological affinity between hydroxyapatite and the underlying bone.

Biomimetic methods of hydroxyapatite coating on Ti are based on the nucleation and growth of calcium phosphate on the surface of implants immersed in simulated body fluid at 37°C. Chemically, the changes occurring on the surface of biomimetic Ti that is subjected to this treatment can be summarized as follows. When subjected to alkaline treatment with NaOH, a hydrogel layer of sodium titanate is formed, which, following the heat treatment, constitutes an amorphous and/or crystalline layer of sodium titanate. Subsequently, during immersion in simulated body fluid, the apatite layer is formed due to the initial precipitation of Ca^{2+} ions that attract phosphate ions PO_4^{3-} [19].

Porous Ti implants subjected to biomimetic treatment were inserted into rabbit tibia in a study by Machado et al. [45]. Observation verified that the mean percentage of bone neoformation in the treated implants, for each of the experimental periods, was higher compared with untreated implants; bone repair showed a statistically significant difference within 15 days. The mechanical test showed that displacement of the coated implants occurred at greater tension values. According to the author, biomimetic treated implants performed better than untreated implants.

According to Nishiguchi et al. [21], the low cost and the effects achieved, including minimizing implant irregularities, make the biomimetic process a better technique than plasma spraying. Furthermore, the authors observed that treatment did not reduce the porosity space available for bone growth, because it causes very little change in the implant surface morphology, affecting approximately 1μm of the surface. Controlling the composition and growth of the apatite film by altering the composition of the simulated body fluid, the incorporation of protein without altering its functions and without the need for heat treatment, are additional advantages of this promising technique [46].

3. Titanium implants obtained by powder metallurgy technique

Titanium is widely used for the production of dental or orthopedic implants because direct contact occurs between bones and implant surfaces [25]. Titanium is biocompatible, highly corrosion resistant and durable. Moreover, it is easily prepared in many different shapes and textures without affecting its biocompatibility [47]. However, most titanium implants consist of dense components, which lead to problems such as bone resorption and implant loosening due to biomechanical mismatch of the elastic modulus [48]. To overcome these problems, porous structures are being investigated extensively, since a reduction in elastic modulus can be coupled with bone integration through tissue ingrowth into pores [49]. The interaction between mechanical behavior and biological processes in cells and tissue is studied in mechanobiology.

Several factors are important for promoting cell growth, such as pore shape and size, as well as their interconnectivity and spatial distribution throughout the implant. Implant architecture is crucial for allowing vascularization and the supply of nutrients to the developing tissue. Studies have shown that the optimum pore size required for implants fixation remains undefined, the consensus is that in order to optimize mineralized bone ingrowth, pore sizes between 100 and 500μm are required [4,5,22]. These porous structures have many applications ranging from spinal fixation to acetabular hip prostheses, dental implants, permanent osteosynthesis plates, and intervertebral discs [50]. In general, porous-surfaced Ti-based implants can be manufactured by one of the following techniques: plasma-spraying [50], anodic dissolution, and grit blasting [33], but these techniques produce only cavities or craters and not interconnected pores. However, there are few efficient techniques for manufacturing these complex shapes with interconnected pores without the need for machining steps [51] such as powder metallurgy (P/M) [4,5,22], the multiple coating technique [52], and powder sintering techniques [53].

The powder metallurgy technique seems to be particularly advantageous because of its processing route and cost [51]. In powder metallurgy, pores can originate from the particle compacting arrangement or from changes in this arrangement, when decomposition of spacer particles causes increasing porosity, and from solid-state diffusion in the sintering step [26]. Finally, the porous structure must also present adequate mechanical strength, since large pores have a deleterious effect on the implant's

mechanical properties. The gradient of maximum porosity must be adjusted adequately with respect to porosity and pore size, in order to ensure the implant's suitable mechanical strength [51,54].

3.1. The powder metallurgy technique

The P/M technique aims to transform metallic powders, using pressure and heat, by means of a thermal treatment (sintering) that substitutes the classic melting and that is carried out below the melting point of the most important metal. The use of the P/M in the biomedical area is recent and its great advantage is the production of prosthesis near to the final format (near net shapes), dense or with controlled porosity and generally less expensive than the conventional processes [4,6].

Titanium powder with different particle sizes can be obtained commercially or by the hydride-dehydride technique (HDH). Hydriding is carried out at 770 K (500°C), in a vertical furnace, for 3 hours, under a positive hydrogen pressure. After cooling to room temperature, the friable hydride is milled in a titanium or niobium container for nearly 30 minutes with argon protecting atmosphere. The dehydriding stage is carried out at 770 K (500°C) in dynamic vacuum conditions.

Porous titanium implants can be manufactured by mixing, in a rolling container for nearly an hour, titanium powder and urea particles as spacer material. Then the powders are uniaxially pressed at 100 MPa into a stainless steel mold and isostatically pressed, using silicone pipe moulds top sealed with plugs, at 200 - 250 MPa. The porous cylindrical samples are heat treated at 453 – 473 K (180 – 200ºC) for 2 h in air to burn out the spacer particles. Sintering is done at 1473 K (1200ºC) for 1 h, under vacuum (10^{-4} Pa (10^{-7} torr)) and free cooling in furnace. Pore size and distribution in the finished implant can be controlled by the particle size and quantity of urea added to the titanium powder.

Dense implants can be obtained by the utilization of powder with optimized size particle distribution which allows better packing during the pressing before sintering. Dense packing of particles is based on selecting particles in such sizes and fractions that voids between larger particles are occupied by successively smaller particles. The remaining porosity is then composed of interstices created by the non-existence of smallest particles in the distribution. Particle size distribution, particle shape, shape factor, surface roughness are some factors that determine final properties of the consolidated powder.

Working with titanium powder obtained by HDH process, starting from titanium sponge, the best densification results after sintering at 1673 K (1400ºC) with 99.8% mean relative density) was obtained for powder milled in a rotative ball mill under vacuum for 36h, that presents a trimodal distribution with higher frequencies for sizes 15 μm, 5 μm and 0.8 μm (Fig. 1). The irregular shape of particles produce an irregular array of voids with the small particles filling voids between the great ones, that enhancing compaction [55].

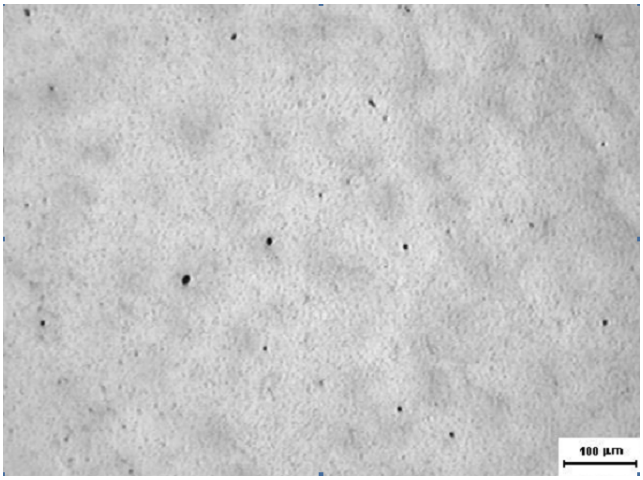

Figure 1. SEM micrography of Ti sample, milled for 36 hours, after sintering at 1673 K (1400ºC), dark points are porous.

3.2. Rough and entirely porous implants

The porous and rough cylindrical implants are fabricated using the powder metallurgy technique. The materials used to manufacture the implants are commercially pure titanium powder with mean particles size of around 80μm, and urea particles around 250 a 350μm in size as spacer material. Titanium/urea powder mixture, in the ratio of 80% weight to 20% weight, respectively, are used to manufacture the porous cylindrical implants and only pure titanium powders are used to manufacture the rough cylindrical implants (Fig. 2). The final implants dimensions are 3.0 mm in diameter and 6.0 mm long [4,5,22].

Figure 2. Cylinders of dense and porous titanium, respectively.

3.3. Surgical procedures

Male New Zealand albino rabbits, aged 6-8 months-old and weighing between 3.5 and 4.0 kg, were used in the studies. The rabbits were provided by the Animal Center of the São José dos Campos School of Dentistry, maintained in individual cages and fed commercial pet food (Coelhil R, Socil) and water ad libitum. These studies were approved by the Research Ethics Committee (044-2002) of the Graduate School of Dentistry of São José dos Campos of São Paulo State University (UNESP).

The implants were cleaned, wrapped and sterilized in autoclave at 393 K (120°C) for 15 min. Prior to surgery, the rabbits were weighed and anesthetized intramuscularly with a mixture of 13 mg/kg of aqueous solution of 2% hydrochloride of 2-(2,6-xylidine)-5,6-dihydro-4H-1,3-thiazine (Rompun®, Bayer, São Paulo, Brazil), an analgesic, sedative and muscular relaxant, and 33 mg/kg of ketamine (Dopalen®, Agibrands do Brazil Ltda., São Paulo, Brazil), a general anesthetic.

The procedures were performed under standard usual sterile conditions. After trichotomy, shaving, and disinfection a straight 3 cm skin incision was made over the medial portion tibiae. a 3 cm longitudinal incision was made over the medial portion of the tibiae, in the proximal cortical bone. The periosteum was carefully detached from the cortical bone and the implantation sites were carefully prepared using an electric surgical drill (AEU707Av2, Aseptico, Washington, USA). The equidistant perforations were made bilaterally and during drilling, the hole was continuously cooled with saline. Just before insertion of the implants, the hole was irrigated with saline to remove any bone shards. The sample was placed in the perforation and pressed into the surgical cavity until it was fixed to the cortical bone. The muscle tissue and skin were sutured with mononylon 4-0 surgical thread (Johnson & Johnson, São José dos Campos, São Paulo, Brazil). Next, all of the rabbits received one dose of antibiotics, 0.35 mg/kg (Pentabiotico®, Fort Dodge Saúde Animal, São Paulo, Brazil). The rabbits were inspected daily for clinical signs of complications or adverse reactions.

The rabbits were sacrificed using an anesthetic overdose administered intramuscularly. Following euthanasia, the surgical segments with the implants were removed and the implants were tested for mobility using a clinical clamp and prepared for histology. The specimens were fixed in 10% formalin. Next, the fragments were embedded in methyl metacrylate (Sigma-Aldrich Chemistry St Louis, MO, USA). Three nondecalcified sections measuring approximately 700μm in thickness were obtained using a diamond saw in a cutting machine for hard tissues (Labcut 1010, Extec, USA). The sections polished (Labpol 8-12, Extec, USA) to a final thickness of approximately 80μm and stained with toluidine blue and histomorphometric analysis was performed using a light microscope (Axioplan 2, Carls Zeiss, Germany) combined with a Sony digital camera (DSC-S85, Cyber-shot). The interfaces were also evaluated by scanning electron microscope (SEM) to characterize the microtopography, morphology and porous interconnection.

The bone formation was evaluated by a blinded investigator, using two different images of both sides of each section of the bone-implant interface, with three sections obtained from each sample taken from each of the rabbits. Thus, numerous images were analyzed, since six fields from each sample were digitized (100x). New bone formation and bone ingrowth into the interior of the pores were calculated using Image J software (NIH, USA). All the quantitative data are expressed as the mean ± standard deviation (SD). Statistical analyses were performed on the histomorphometric results of bone ingrowth depth using a randomized block design ANOVA, with a post-hoc Tukey test ($p=0.05$), to determine the differences between sample conditions.

After each sacrifice period, the bone fragments of rabbits, containing the implant were preserved in distilled water in a freezer at 253 K (-20ºC) until the mechanical testing, which was performed at room temperature. For the push-out test, each specimen was mounted on a special platform with a central circular opening. This jig was designed to maintain the pushing load parallel to the long axis of the implant. The pushing load was applied to the end of the implant using a universal testing machine (Instron 2301) at a cross-head speed of 0.5 mm/min until the peak load was obtained.

It is necessary to determine the area to which the force was applied to determine the shear stress needed to displace the implant. Therefore, the cortical thickness of each specimen was measured at three locations for each push-out sample. The mean thickness was calculated and used to determine the contact area according to the following formula: mean area (Am) = $2\pi r$ x mean cortical thickness, where r = implant radius. Next, the shear stress was calculated using the equation: $\tau = F/Am$, where τ = shear stress; and F = peak load at failure. Statistical analyses was performed on the values obtain in the push-out test by a randomized block design ANOVA, with a post-hoc Tukey test ($p<0.05$), to determine the differences between sample conditions. Cylindrical implants with porous surface were compared to cylindrical implants with rough surface regarding the quantity and quality of new bone formation on the implant-bone interface after implantation in rabbit tibiae.

As results, all animals presented satisfactory postoperative results, without any evidence of inflammation or infection in the surgical site. No adverse reaction was observed during the procedure. During the clinical evaluation, the implants were not loose manually. The appearance of the surrounding tissue and healing in the implantation site were examined, and any mobility of the sample or other abnormalities were noted.

The results showed that all implants were well tolerated and osseointegration was observed in both groups with no difference of new bone quality. However, when the quantity of bone neoformation at implant-bone interface was evaluated, a larger formation of bone tissue was observed for the porous-surface implants, and this difference was statistically significant. This results point out that the cylindrical porous-surface implants yielded greater bone neoformation than the cylindrical rough-surface implants because of their larger area in contact with the bone tissue and the presence of an intercommunicating porous structure that allowed the formation of a three dimensional osseointegration network.

The micrography of the porous cylindrical implants showed different types of pores, interconnected pores and few isolated pores. The average interconnected pore diameter was about 480μm (± 210), and 37% (± 2.0) total porosity. The micrography of the rough cylindrical implants showed only isolated smaller pores, with average pore diameter of about 180μm (± 80) and 3% (± 0.8) total porosity. The rough cylindrical implants presented an average surface roughness of Ra 5.30μm.

At 4 and 8 weeks, new bone was observed at the implant–bone interface, regardless of the type of implant, leading to an osseointegration (Fig. 3), and in the porous implants new bone was also noticed into the pores. This new bone was similar in the two periods of sacrifice; it was constituted of mature bone trabeculae that presented lamellar arrangement and of different size medullar spaces. There was, especially in the rabbits sacrificed in the 4 weeks period, a distinct border between newly formed bone and preexisting bone (Fig. 4), emphasizing the biocompatibility of the material and the adequate surface to new bone proliferation.

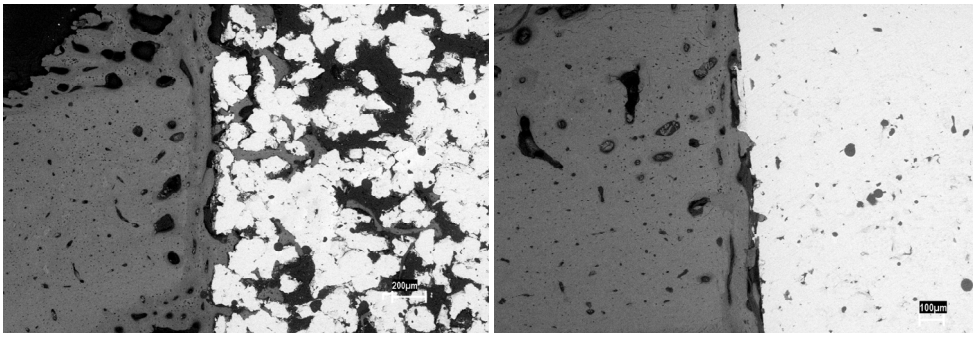

Figure 3. SEM micrography of (left)porous implants with bone ingrowth and (right) rough implant. Both 4 weeks after surgery, note a distinct border between new bone and preexisting bone (arrow)

Bone ingrowth was observed in all animals that received porous implants. Regardless of the sacrifice period, bone ingrowth into the pores was observed, even into more internal pores. In general, for both periods the small pores were totally filled with bone, whereas in the 4-week period bigger pores presented partial filling, and in the 8-week period bigger pores were total filling. New bone was also observed above the implants and in the inferior region of the implants and the pores of these areas also presented new bone (Fig. 4). No fibrous tissue was observed on the interface regardless of the implant type or sacrifice period.

The mean values obtained for the percentage of implant–bone contact in the porous versus the rough cylindrical implants were, respectively, 57% (0.7%) vs. 46% (0.9%) after 4 weeks, and 59% (1.3%) vs. 50% (0.8%) after 8 weeks.

Additionally, in this study, the shear strengths of porous and rough implants 4 weeks postsurgery were 14 MPa (1.1 MPa) and 4 MPa (1.8 MPa), respectively. At 8 weeks, the shear

strength was greater, 20 MPa (2.3 MPa) for porous implants and 13 MPa (0.95 MPa) for rough implants. Observation also verified that, regardless of the implant type, shear strength increased as the experimental period increased. The porous implants of the rabbits euthanized at 8 weeks of bone repair exhibited the greatest shear strength values. Therefore, bone ingrowth into pores provides a more effective fixation of porous implant to bone, due to the development of resistant areas to shear strength. These resistant areas were directly related to the quantity of open pores in the surface. Thus, in order to occur the dislodging of porous implant, the fracture of bone that proliferated into pores was necessary.

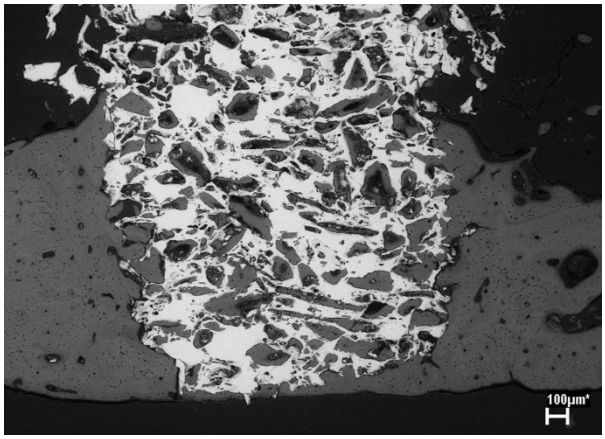

Figure 4. SEM micrography of porous titanium scaffold 4 week period showing new bone growth in the region above the implant and in the inferior region and pores.

The powder metallurgy technique was efficient in producing porous titanium implants and dense titanium samples for biomedical applications. This technique allows for the preparation of implants with interconnected pores resembling a three-dimensional network and the control of pore size and porosity, through the selection of appropriate spacers, providing excellent implants for bone ingrowth.

Finally, an important prospective clinical use for porous implants is the manufacture of short implants for clinical situations such as cases of limited available bone height, poor quality bone [56,57], or orthodontic loading [58]. The small segment of porous implant allowed an effective osseointegration, due to increased contact area provided by its surface configuration. The porous implants of this study were manufactured with dimensions that could be used in these dental clinical situations, since they presented small diameter and height, and exhibited threedimensional bone ingrowth and mechanical interlocking.

3.4. Dense implants with a porous coating

Porous structures were produced by powder metallurgy techniques. The pure titanium grade 2 powder (Micron Metals, EUA) by HDH process coatings were placed over rod

substrates of Ti-6Al-7Nb (Fig. 5) with 5.8 μm medium roughness (Ra), produced by powder metallurgy. Titanium powders were mixed with different quantities of urea as a binder, in order to produce a high porosity level. Both titanium and urea powders were separated in narrow particle size range in order to control de medium pore sizes and total porosity. The powder ranges were 144 – 177μm for titanium and 500 a 590μm for urea. A size range of < 840μm for urea was also used for comparison. Coatings specified as C1, C2 and C3 were processed from titanium powders, mixed with 30%, 40% and 50% weight of urea respectively [59].

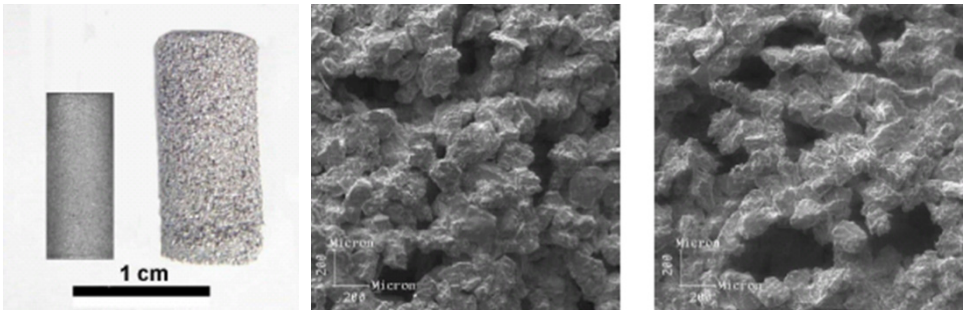

Figure 5. (a) Macrophotography of the Ti-6Al-7Nb substrate and a coating on substrate sample; (b) and (c) SEM surface topographic images for the coating-substrate samples C1-30% urea and C3-50% urea, respectively

Cold isostatic compaction (CIP) was performed using silicone pipe moulds top sealed with plugs. For the coatings samples, the substrates were centered in the mould and the mixtures were then tapered. Compaction pressure was 250 MPa for all samples. The compacted samples were heat-treated in a muffle for complete elimination of the binder. Then they were sintered in a high vacuum furnace (10^{-3} Pa (10^{-6} torr)), one hour step at 1473K (1200ºC) and free cooling in furnace.

All samples exhibits open macroporosity in the range of 100 – 800μm and closed microporosity in the range of 1 – 50 μm. The macropores were originated from the binder evaporation while the micropores can be related with the porous nature of the titanium powder and the low compaction pressure used (250 MPa) which doesn't lead to a high densification after sintering. Measured coating thickness was in the range of 750 – 955μm.

The influence of the binder parameters in the sample porosity was succeeded. Pore volume fractions ranges where coherent with the percent binder additions, for both types of samples. Foam samples exhibited less volume fraction of pores than the coatings made with the same binder additions. The coatings presented many regions linked with the substrate, indicating a qualitatively strong bond of the coating. The similarity of the pore size distribution for coatings and foams samples indicates a good reproducibility of the porous structures [59].

3.5. Dense core implants with an integrated porous surface

Several porous coating fabrication methods have been proposed, including sintering uniform-sized beads, fibers by isostatic press sintering, sintering loosely packed powders, the atomization process and powder metallurgy on a dense core. Materials produced by these methods present an interface between the dense core and porous coating [8,60-63]. To overcome this problem a new method to produce titanium samples was to develop, that exhibit a dense core with an integrated porous surface, reducing the problems of displacing a porous coating [6,7,64].

Titanium samples were produced with a dense core and porous surface in one step, using a purpose-designed stainless steel mold. The porous surface titanium samples were prepared using pure Ti powders developed in the General Command of Aerospace Technology (CTA), Institute of Air and Space (IAE), Division of Material (AMR), Brazil (purity ≥ 99.5%, particle size ≤ 8μm), which were formed by HDH process. An organic additive (urea) was used as a space holder. The weight ratio of Ti powder to space-holder was calculated to obtain defined porosities of 30 and 40% in the sintered compact samples. The powder Ti and space particles were mixed in a rolling container for an hour. By controlling the quantity and size of the spacer particles, we fabricated three different porous surfaces with different porosities and pore sizes: Group 1 - 30% pores with an average pore diameter of 180μm; Group 2 - 30% pores with an average diameter of 300μm, and Group 3 - 40% pores with an average diameter of 180μm.

All the samples used in this study were fabricated through cold compaction using a manually operated uniaxial press. Initially, the Ti powder was compacted into a central tube of purpose-designed stainless steel mold. Then, the mixture was inserted around the central tube and strongly compacted. Previously to uniaxial press, the central tube was removed, and the stainless steel mold was uniaxially pressed at 500 MPa. Green samples were obtained by cold isostatic pressing at 300 MPa and heat-treated on a stove to eliminate urea. The sintering process consisted of two steps and it was performed on a vacuum furnace (10^{-4} Pa (10^{-7} torr)). The first step included heating stage at 1473 K (1200ºC) with heating rate of 293 K (20ºC)/min. In the second step the samples were maintained at 1473 K for 1 h. After sintering, the samples presented 4 mm diameter and 6 mm long (Fig. 6).

The surface morphology and porous structures were evaluated by optical quantitative metallography and the Image Tool software. The cylindrical samples were previously divided into 5 sections, and 4 images of each section were captured, totaling 20 images of each sample, which were taken at 100X magnification. Porous surface microstructure and topography were characterized by scanning electron microscopy (SEM). Prior to implantation, porous surface titanium samples were cleaned by ultrasonic action for 30 min in a 1% (v/v) detergent/distilled water (dH_2O) solution, and then rinsed 3 times in dH_2O. Following cleaning, the samples were packaged in sterilizable pouches and sterilized in an autoclave at 394 K (121ºC) for 15 min.

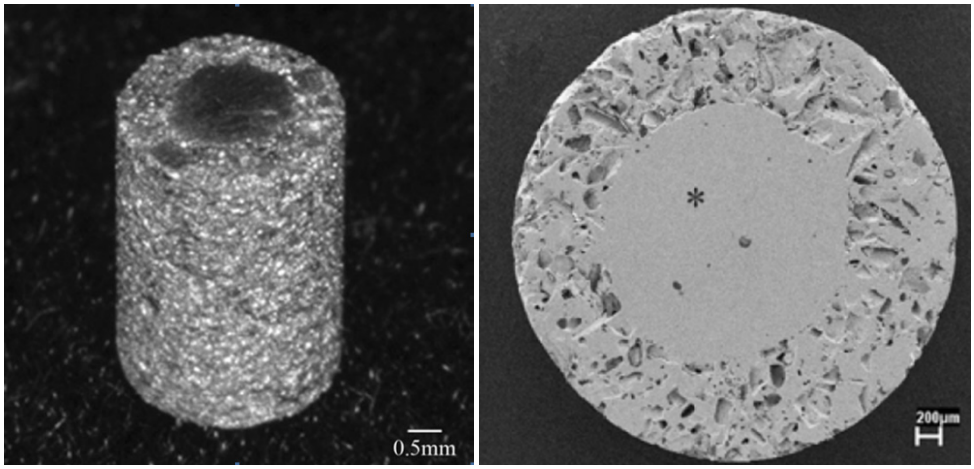

Figure 6. Figure 6- Visual aspect of titanium sample, and cross section, with a dense core with an integrated porous surface, fabricated by a powder metallurgy technique.

The implants were surgically inserted into thirty rabbits, that received a total of 6 porous surface titanium samples in the cortical bone beds of the proximal left and right tibia, so each tibia received 3 samples, with one of each group (G1, G2, G3). All animals were given a dose of antibiotic and were monitored until sacrifice at 8 and 12 weeks after implantation. Following euthanasia, the six rabbits surgical segments with the implants were removed and submitted to histological and histomorphometric analysis.

Osseointegration was evaluated by a blinded investigator, using 2 different images of both sides of each section of the bone-implant interface, with three sections obtained from each sample taken on each of six different rabbits. Thus, 72 pictures were analyzed, since six fields of each sample were digitized (100X), and each animal received two samples of each group (G1, G2, G3). New bone formation and bone ingrowth into the interior of the pores were calculated using Image J software (NIH). Shear mechanical tests (push out) were performed to evaluate the implant removal resistance.

All quantitative data were expressed as a mean ± standard deviation (SD). Statistical analyses were performed on compression test values, on histomorphometrical results of bone ingrowth depth and on values of the push-out test by a randomized block design ANOVA with a post hoc Tukey test (5%) to determine differences between samples conditions.

The structure of the sample observed by SEM is presented in Fig. 7, and it was not observed line fracture or any discontinuity in the transition region of the different structures of Ti (porous/dense). The porous structure exhibited different types of pores, with interconnected macro and micropores.

The bone ingrowth percentages are presented in Table 1. All of the rabbits presented satisfactory postoperative results. There were no surgical complications and all implants

were firmly attached to the bone. No macroscopic or microscopic signs of infection were found, and during clinical evaluation, the implants could not be loosened manually. New bone was observed at the implant-bone interface (Fig. 8), regardless of the type of sample, leading to osseointegration, and new bone was also observed growing into the pores (Fig. 9). This new bone consisted of mature bone trabeculae that presented lamellar arrangement and different-sized medullary spaces. Regardless of the sacrifice period, bone ingrowth into the pores was observed in all implants, even deep inside the more internal pores (Fig. 9). In general, the smaller pores were totally filled with bone, whereas bigger pores were partially filled. No fibrous tissue was observed at the interface, regardless of the sample type or sacrifice period.

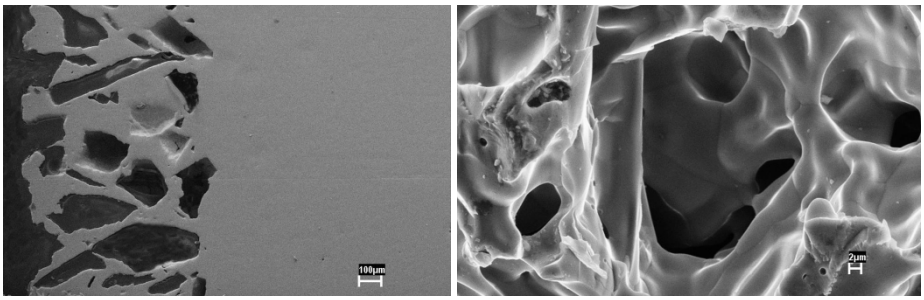

Figure 7. Scanning electron images of a longitudinal section showing a dense core with an integrated porous surface and interconnected pores, micropores and macropores.

SP (weeks)[a]	Implants		
	G1	G2	G3
8	59,460 ± 7,980	72,814 ± 8,936	72,146 ± 6,430
12	60,540 ± 8,310	73,006 ± 9,760	72,714 ± 7,020

[a] Sacrifice period

Table 1. Average bone ingrowth (%)

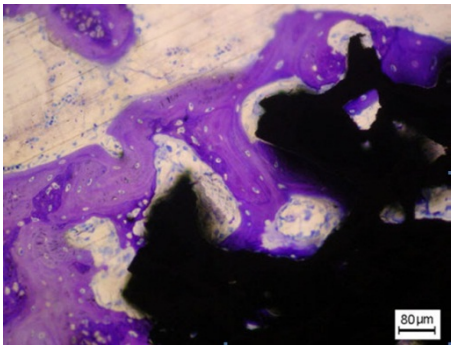

Figure 8. Histological optical image stained with toluidine blue: osteocytes in the lacunae, new bone proliferation, osteoid matrix, and osteoblasts.

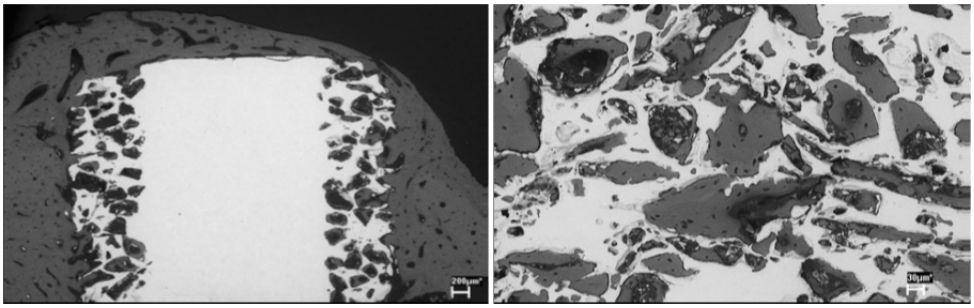

Figure 9. SEM micrograph of the bone-sample interface: osseointegration and new bone ingrowth into a porous surface as far as the more internal pores near to the dense core.

The values obtained for the percentage of bone ingrowth into the available space inside the implants with different pores and porosities were not significantly different at 8 and 12 weeks post-implantation. However, statistically significant differences were determined among the implant types ($p<0.01$), with group 1 (30% pores/180 μm) presenting the lowest quantities of new bone and group 2 (30% pores/300 μm) showing the greatest quantity of new bone. The mean value for bone-implant contact percentage was 72.43% (±6.89) for group 3 (40% pores/180 μm) and 72.91% (±9.62) for group 2. These values were lower in group 1, which demonstrated bone ingrowth of 60% (±8.54) into the available space inside the implants.

The shear strengths of all groups exhibited statistically significant differences when the implant type ($P<0.05$), sacrifice period ($P<0.001$) and interaction effect ($P<0.05$) were analyzed. Group 2 presented the lowest shear strength at 8 weeks (9.05 MPa), while group 3 presented the greatest shear strength at 12 weeks (16.63 MPa) (Table 2).

SP (weeks)[a]	Implants		
	G1	G2	G3
8	11.67 ± 1.941	9.05 ± 2.940	10.34 ± 3.270
12	11.18 ± 3.600	11.66 ± 4.020	16.63 ± 5.110

[a] Sacrifice period

Table 2. Average shear strength (MPa)

Not surprisingly, in this current experiment, the observations revealed the smallest amount of bone neoformation at the bone-implant interface in Group 1 samples when compared with the other groups. This phenomenon was attributed to the association of porosity percentage with pore areas, since this combination in G2 and G3 groups permitted greater vascularization and subsequent differentiation, improving bone ingrowth.

Increasing both area and complexity of the surface improves the mechanical interlocking and can increase the implant stability. This provides a mechanical interlocking, a mechanism that is not observed on flat or rough surfaces.

Mechanical shear testing verified that Group 2 samples showed the least resistance to displacement (9.05 MPa) at 8 weeks, probably because of their larger pore size, which were not entirely filled by bone at 8 weeks, and their lower porosity. In contrast, At 12 weeks, while Groups 1 and 2 showed similar resistance, Group 3 implants showed the greatest resistance to displacement (16.63 MPa), probably due to their structure with high porosity. Its high porosity provided more area for bone ingrowth at the interface, since the rupture of the bone ligaments grown into the interface pores are the main resistance source to the shear stresses generated in the push out test.

Titanium sample exhibiting a dense core with an integrated porous surface developed and characterized in this current study is unique and different of standard structures used in orthopedic or dentistry implants. The porous surfaces were fabricated using a powder metallurgy technique in one step, using a purpose-designed stainless steel mold, instead of produced by sintered beads on a dense core. This new method reduces the problems of displacement of the porous coating. Three types of porous surface titanium implants with varying pore diameters and porosities were fabricated by powder metallurgy in one step and all specimens presented an interconnected, complex porous structure and dense core. Bone ingrowth into the pores was observed in all implants, even deep inside the more internal pores.

3.6. Porous implants with biomimetic coating

Titanium implants can also be bioactivated by a biomimetic precipitation process which is an alternative for other coatings methods. The biomimetic process is employed both to identify the material ability to form calcium phosphate *in vitro* (biocompatibility evaluation) and to obtain calcium phosphate coatings on metallic substrates. The process advantages compared to other process are: the low temperature, which is usable to any heat sensitive material, formation of bonelike apatite crystals with high bioactivity, deposition on and into porous surfaces without changing the pore morphology, good adhesion to the substrate and the possibility of bone growth stimulating factors incorporation [65].

Chemical composition and surface topography are important parameters influencing the mechanical bond between bone and implant. The biomimetic process promotes a Calcium

phosphate (CaP) film deposition by immersion of the porous titanium part in a simulated body fluid [19,65]. CaP coatings onto metallic biomaterials have gained great interest, due to the chemical interactions between the coated surface and the biological tissues. CaP coatings also enhance biocompatibility, associated to the good mechanical properties of the metallic substrate, stimulating osseointegration [66-68].

Porous titanium cylindrical samples (8mm diameter x 5mm length) were prepared using a titanium powder grade 2 with particle size range of 149 - 177μm and manufactured by HDH-hydrogenation-dehydrogenation process. Urea with 250 - 297μm was used as an organic additive for pore formation. The powders were mixed in a proportion of 70% and 30% respectively, encapsulated in silicone molds which were tapered and sealed. Thereafter, cold isostatic pressing was performed at 300 MPa. For the elimination of the organic additive, the samples were heat treated on a stove at 473 K (200°C) for 2 hours. Compacted samples were sintered in a vacuum furnace (10^{-4} Pa (10^{-7} Torr)) at 1473 K (1200°C) for 1 hour and later were cleaned with deionized water [45].

Samples were submitted to biomimetic treatment, beginning with alkali treatment of the samples in NaOH (10M) at 403 K (130ºC) in an autoclave (Fanem (London - SP) for 1h, followed by heat treatment at 473 K (200ºC) for 1 hour and immersion in a solution of modified simulated body fluid (mSBF) at 37°C. The mSBF solution used to accomplish the biomimetic process was: $[Na^{-}]$ = 142.0 mM; $[K^{-}]$ = 5.000 mM; $[Mg^{-2}]$ = 1.500 mM; $[Ca^{-2}]$ = 2.500 mM; $[Cl^{-}]$ = 147.8 mM; $[HCO_3^{-}]$ = 4.200 mM; $[HPO_4^{-2}]$ = 1.000 mM and $[SO_4^{-2}]$ = 0.050 mM; a modification proposed by Andrade et al. The pretreated samples were immersed in mSBF solution with pH 7.4 at 310 K (37 ºC) for 14 days. The solution was renewed every two days. After the immersion period, the samples were cleaned with deionized water, dried in air sterilized by ionizing radiation 20KGF prior to use. No treated implants were used as controls.

The implants were surgically inserted into thirty rabbits, with three coated implants in the left tibia and three untreated/control implants in the right tibia. All animals were given penicillin and were monitored until sacrifice 15, 30 and 45 days after surgery. After euthanasia, the surgical segments with the implants were removed and submitted to histological and histomorphometric analysis. Shear mechanical tests (push out) were performed to evaluate the implant removal resistance.

Microstructural analyses were performed by Scanning Electron Microscopy (SEM), Electron Dispersive X-Ray Spectroscopy (EDS) and Raman Spectroscopy. Evaluation of the bone tissue neoformation was conducted by SEM and optical microscopy (OM), by comparison between coated and uncoated implants.

SEM analysis has shown an implant surface without treatments with small closed micropores (< 50 μm) and interconnected macropores from 100 – 500 μm (Fig. 10a, 10b). Figure 14c shows a pretreated sample, which exhibited needle-like sodium titanate (Na_2TiO_3) crystals (Fig. 10c). After fourteen days under biomimetic treatment, samples presented globular formations, associated with the deposition of a CaP film (Fig 10d).

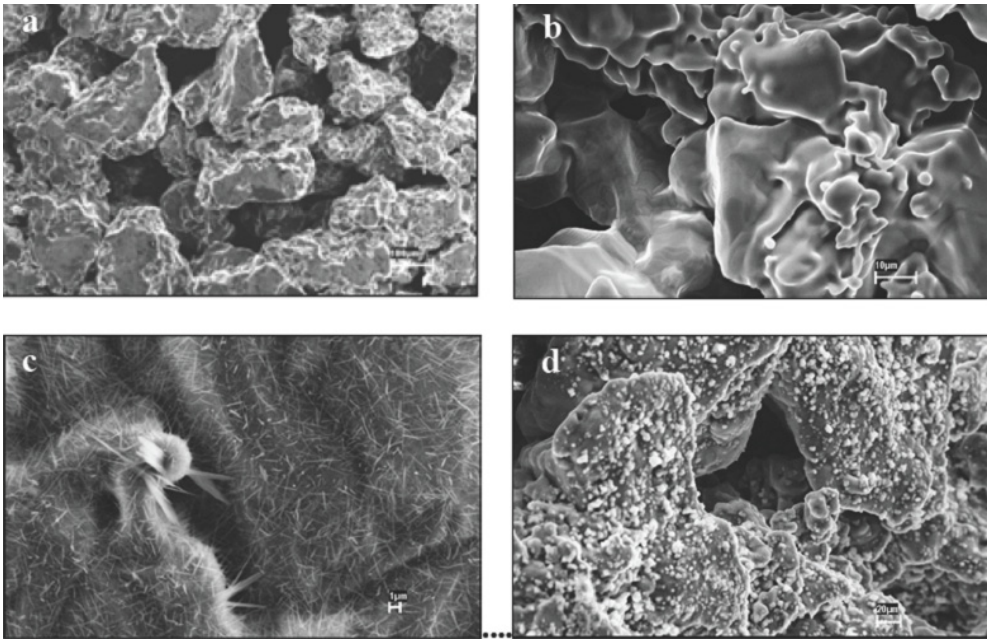

Figure 10. SEM images of a control implant, without treatments (a, b), after treatments (c) and with biomimetic coating (d).

EDS analysis showed high peaks of Ca and P at the surface of the implants (Fig. 11 left), while Raman spectra evidenced a 960 cm-1 peak, characteristic of hydroxyapatite (Fig. 11 right).

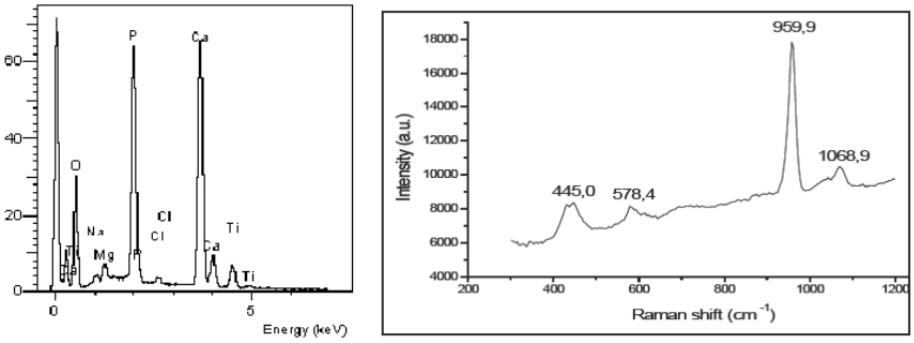

Figure 11. EDS (left) and Raman (right) spectra after biomimetic treatment

SEM images and optical micrographs (Fig. 12) revealed the bone tissue neoformation at the bone-implant interface which was also detected inside the pores, including internal ones. This result evidenced the osseointegration of the designed CaP-coated titanium implant.

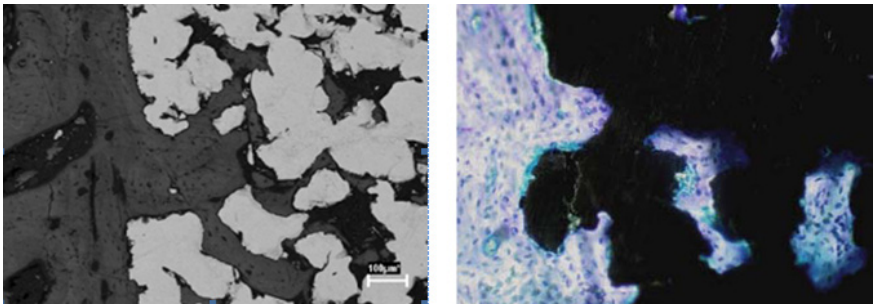

Figure 12. SEM image of tibiae sample evidencing the bone ingrowth into the surface pores and an optical micrograph of tibiae sample evidencing the bone-implant interface and bone ingrowth into de pores.

Table 3 lists the bone neoformation in rabbits'tibiae measured at 15, 30 and 45 days.

Time (days)	Test group (%)	Control group (%)
15	37.45 ±2.26	32.26 ±3.18
30	37.91±5.44	37.13±3.57
45	38.37±6.32	37.18±6.05

Table 3. Mean bone neoformation in rabbits'tibiae.

Displacement resistance values of the implants from bone of the test and control groups, are listed in Table 4.

Time (days)	Test group (MPa)	Control group (MPa)
15	7.30 ±1.63	6.36 ±3.48
30	19.24±2.89	12.88±2.51
45	19.48±3.35	15.65±3.32

Table 4. Shear test results: displacement resistance (MPa) of the implants from bone.

The biomimetic coating treatment induced the formation of hydroxyapatite on the porous Ti implant surfaces. The coated implants presented better osseointegration than the implants without coating, being bone neoformation enhanced in the period of 15 days after surgery.

The biomimetic process can be considered as an experimentally simple and viable alternative to obtain osseoconductive coatings of calcium phosphate onto metallic substrates, especially titanium.

3.7. Human osteoblast response to porous titanium with biomimetic coating

In vitro evaluation of osteoblast response is widely used to explain the phenomena of osseointegration to Ti. Papers describe osteoblast-like MG-63 cultures [39,40]. One of the main criticisms of these studies is the use of immortal osteosarcoma cells.

To conduct research involving human cell cultures, approval is required from the institute's Ethics Committee on Human Research and must include donor signatures on a term of free, informed consent.

During different surgical procedures on the maxillary bones that require drilling, regularization of the alveolar interradicular and/or interdental crests, the dental surgeon removes bone fragments that are discarded. Instead of disposing of these, such fragments can be prepared as described below to obtain osteoblast cell cultures.

The osteogenic cells are isolated by enzymatic digestion of tissue fragments of human alveolar type II collagenase (Gibco-Life). Cells and explants are cultured for up to 14 days in Minimum Essential Medium alpha modification (α-MEM), supplemented as previously described (Rosa et al. 2009) at 37°C in a humid atmosphere containing 5% CO_2. Titanium samples biocompatibility may be analyzed with these cells.

Titanium disks were fabricated by powder metallurgy, using a 12mm diameter, 5mm thick matrix. The porosities were determined by mixing proportions of 80% Ti and 20% urea and 70% Ti and 30% urea, the organic additive used as a spacer. Each porous sample used 1 g of the mixture, which was fabricated, by powder metallurgy, as described above. Urea particle size determined a pore diameter of 300μm.

Six experimental groups were outlined: a) control, a dense Ti sample; b) a lower porosity Ti sample; c) a higher porosity Ti sample; d) a dense Ti sample + biomimetic treatment; e) a lower porosity Ti sample + biomimetic treatment; and f) a higher porosity Ti sample + biomimetic treatment.

Dense Ti sample density was determined first, following measurements of mass, diameter, height, using the density formula. The density obtained (4.40 g/cm^3) was similar to that classically described in the literature (4.50 g/cm^3). Next, the porous Ti samples were subjected to the same measurements and porosity percentage was determined, considering all the void space as pores. The lower porosity group presented 33±1.69% and the higher porosity group presented 41.4±1.93% porosity. Half of the samples were submitted to biomimetic treatment as described previously. The presence of calcium phosphate in the biomimetically treated samples was observed in the form of whitish granules or flakes on the surface of the pores. Analysis was also performed by X-ray diffraction, which detected the crystal structure of the hydroxyapatite (calcium phosphate) layer.

The results of cell adhesion, alkaline phosphatase activity, total protein content and cell growth or cell viability *in vitro* obtained in this study are shown in Figure 13.

ANOVA and Tukey tests verified that the percentage of adherent cells and alkaline phosphatase activity were similar in all the Ti samples, independent of porosity and the presence of biomimetic coating (Fig. 13). However, phosphate hydroxide deposition in samples with biomimetic treatment reduced the total protein content and viability of the cells tested. Analyzing cell behavior based on the results obtained in this study, we conclude that the biomimetic treatment impaired Ti biocompatibility. Mammalis et al [69] also found

that chemical modification decreases cell attachment and proliferation. It is possible that the physical presence of calcium phosphate granules damages cells in culture. This has not occurred *in vivo*, most likely due to the fibrin network, and our group has reported good results with biomimetic coating [45].

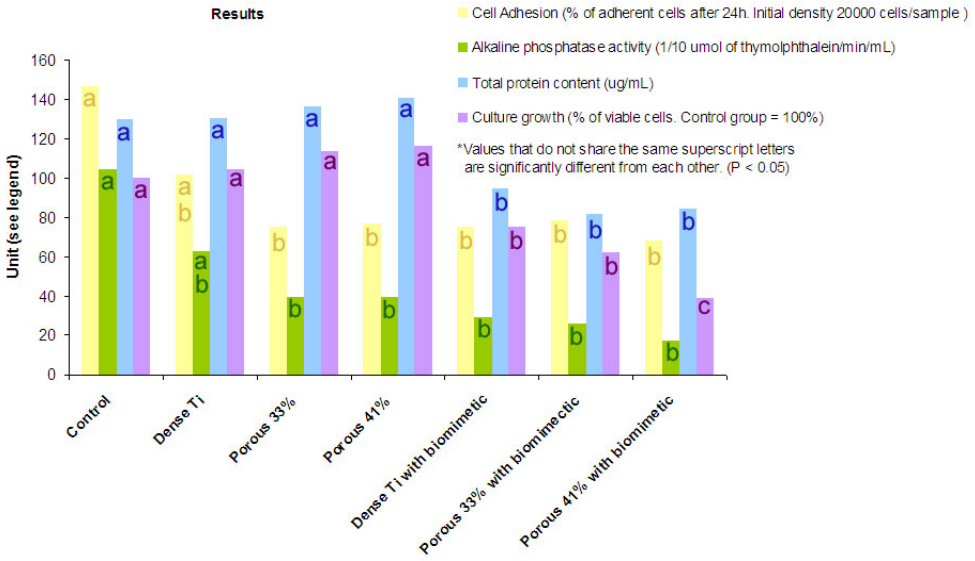

Figure 13. *In vitro* effects of porosity and biomimetic treatment in titanium samples

4. Conclusion

Titanium porous implants with interconnected porous structure were successfully prepared by powder metallurgy techniques by using grounded HDH titanium powder. Porous size and porosity can be controlled by space material characteristics prior to powder mixture. The porous structure enhances the bone formation, ingrowth and the implant displacement resistance. Dense core with integrated porous surface titanium implants were manufactured by one step compacting method seems to be a promising approach for bone tissue engineering. The implant porous region behaviors like a titanium/bone composite in order to accommodate the tensions due the mismatch of elastic modulus. Despite the conflicting results, the hydroxyapatite coating through biomimetic treatment merits further study because of the improved osseointegration obtained *in vivo*.

Author details

Luana Marotta Reis de Vasconcellos and Yasmin Rodarte Carvalho
Department of Bioscience and Oral Diagnosis,
São Jose dos Campos School of Dentistry Univ. Estadual Paulista (UNESP), Brazil

Renata Falchete do Prado, Mário Lima de Alencastro Graça and Carlos Alberto Alves Cairo
Department of Materials – Aeronautical and Space Institute,
Aerospace Science and Technology Department, Brazil

Luis Gustavo Oliveira de Vasconcellos
Department of Prosthodontics and Dental Materials, São Jose dos Campos,
School of Dentistry, Univ. Estadual Paulista (UNESP), Brazil

Acknowledgement

The authors would like to thank the São Paulo Research Foundation (FAPESP) for the grants required to complete this work.

5. References

[1] Park JB, Lakes RS (1980) Biomaterials: an introduction. New York: Plenum Press. 561p.
[2] Teixeira E.R. (2004) Superfície dos implantes: o estágio atual. In: Implantes Osseointegrados: cirurgia e prótese. Dinato JC, Polido WD. São Paulo:Artes Médicas. pp. 63-80.
[3] Bhattarai SR, Khalil KA, Dewidar M, Hwang PH, Yi HK, Kim HY. (2008) Novel production method and in-vitro cell compatibility of porous Ti-6Al-4V alloy disk for hard tissue engineering. J. biomed. mat. res. A. 86: 289-299.
[4] Vasconcellos LM, Oliveira MV, Graça ML, Vasconcellos LG, Cairo CAA, Carvalho YR. (2008(a)) Design of dental implants, influence on the osteogenesis and fixation. J. mat. sci.: mat. med. 19: 2851-2857.
[5] Vasconcellos LM, Oliveira MV, Graça MLA, Vasconcellos LGO, Cairo CAA, Carvalho YR. (2008(b)) Porous titanium scaffolds produced by powder metallurgy for biomedical applications. Mat. res. 11: 275-280.
[6] Vasconcellos LM, Leite DO, Nascimento FO, Vasconcellos LGO, Graça MLA, Carvalho YR, Cairo CAA. (2010(a)) Porous titanium for biomedical applications - An experimental study on rabbits. Med. oral patol. oral cir. bucal. 2: E407-412.
[7] Vasconcellos LM, Leite DO, Nascimento FO, Carvalho YR, Cairo CAA. (2010(b)) Evaluation of bone ingrowth into porous titanium implant: histomorphometric analysis in rabbits. Braz. oral res. 24: 399-405.
[8] Wazen RM, Lefevre L-P, Baril E, Nanci A (2010) Initial evaluation of bone ingrowth into a novel porous titanium coating. J. biomed. mat. res. B: applied biomat. 94: 64-71.
[9] Bottino MC, Coelho PG, Henriques VA, Higa OZ, Bressiani AH, Bressiani JC (2009) Processing, characterization, and in vitro/in vivo evaluations of powder metallurgy processed Ti-13Nb-13Zr alloys. J. biomed. mater. res. A. 88: 689-696.
[10] Bottino MC, Coelho PG, Yoshimoto M, König Jr B, Henriques VAR, Bressiani AHA, et al. (2008) Histomorphologic evaluation of Ti-13Nb-13Zr alloys processed via powder metallurgy. A study in rabbits. Mat. sci. engin. C. 28: 223-227.

[11] Santos DR, Pereira MS, Cairo CAA, Graça MLA, Henriques VAR (2008) Isochronal sintering of the blended Elemental Ti-35Nb alloy. Mat. sci. eng. A. 472: 193-197.

[12] Rosa AL, Crippa GE, Oliveira PT, Taba MJ, Lefebvre LP, Beloti MM. (2009) Human alveolar bone cell proliferation, expression of osteoblastic phenotype, and matrix mineralization on porous titanium produced by powder metallurgy. Clin. oral implant res. 20: 472–481.

[13] Callister WD (2007). Propriedades mecânicas dos metais. In: Callister WD, Willian D. Ciência e Engenharia de Materiais: uma introdução. Rio de Janeiro: LTC. pp. 131-168.

[14] Dewidar M., Yoon HC, Lim JK. (2006) Mechanical properties of metals for biomedical applications using powder metallurgy process. Met mat int. 12: 193-206.

[15] Laheurte P, Prima F, Eberhardt A, Goriant T, Wary M, Pattor E. (2010) Mechanical properties of low modulus beta titanium alloys designed from the electronic approach. J. mec. behav. biomed. mat. 3: 565-573.

[16] Santos DR, Henriques VAR, Cairo CAA, Pereira MS. (2005) Production of a low young modulus titanium alloy by powder metallurgy. Mat. res. 8: 439-442.

[17] Andrade MC, Sader MS, Filgueiras MR, Ogasawara T. (2000) Microstructure of ceramic coating on titanium surface as a result of hydrothermal treatment. J. mat. sci. mat. med. 11: 751-755.

[18] Kim HM, Kokubo T, Fujibayashi S, Nishiguchi S. Nakamura T. (2000) Bioactive macroporous titanium surface layer on titanium substrate. J. biomed. mat. res. 52: 553-557.

[19] Kokubo T, Miyaji F, Kim HM, Nakamura T. (1996) spontaneous formation of bonelike apatite layer on chemically treated titanium metals. J. am. ceram. soc. 79:1127-1129.

[20] Nguyen HQ, Deporter DA, Pilliar RM, Valiquette N, Yakubovich R (2004) The effect of sol-gel formed calcium phosphate coatings on bone ingrowth and osteoconductivity of porous-surfaced Ti alloy implants. Biomaterials. 25: 865-876.

[21] Nishiguchi S, Kato H, Neo M, Oka M, Kim HM, Kokubo T, Nakamura T. (2001) Alkali- and heat-treated porous titanium for orthopedic implants. J. biomed. mat res. 54: 198-208.

[22] Brentel AS, Vasconcellos LM, Oliveira MV, Graça ML, Vasconcellos LG, Cairo CA, Carvalho, YC. (2006) Histomorphometric analysis of pure titanium implants with porous surface versus rough surface. J. appl. oral sci. 14: 213-218.

[23] Faria PEP, Carvalho AL, Felipucci DNB, Wen C, Sennerby L, Salata LA. (2010) Bone formation following implantation of titanium sponge rods into humeral osteotomies in dogs: a histological and histometrical study. Clin. implant dent. rel. res. 12: 72-79.

[24] Frosch KH, Barvencik F, Lohmann CH, Viereck V, Siggelkow H, Breme J, Dresing K, Stürmer KM. (2002) Migration, matrix production and lamellar bone formation of human osteoblast-like cells in porous titanium implants. Cell tis. org. 170: 214-227.

[25] Branemark PI. (1983) Osseointegration and its experimental background. J. Prosth. Dent. 50: 399-410.

[26] Ryan G, Pandit A, Apatsidis DP. (2006) Fabrication methods of porous metals for use in orthopaedic applications. Biomaterials. 27: 2651-70.

[27] Xue W, Krishna BV, Bandyopadhyay A, Bose S. (2007) Processing and biocompatibility evaluation of laser processed porous titanium. Acta biomater. 3: 1007-1018.

[28] Karageorgiou V, Kaplan D (2005) Porosity of 3D biomaterial scaffolds and osteogenesis. Biomaterials. 26: 5474-5491.

[29] Götz HE, Müller M, Emmel A, Holzwarth U, Erben RG, Stangl R. (2004) Effect of surface finish on the osseointegration of laser-treated titanium alloy implants. Biomaterials. 25: 4057-4064.

[30] Liu YL, Schoenaers J, Groot K, Wijn JR, Schepers E. (2000) Bone healing in porous implants: a histological and histometrical comparative study on sheep. J mat. sci mat. med. 11: 711-717.

[31] Kujala S, Ryhänen J, Danilov A, Tuukkanen J. (2003) Effect of porosity on the osteointegration and bone ingrowth of a weight-bearing nickel-titanium bone graft substitute. Biomaterials. 24: 4691-4697.

[32] Takemoto M, Fujibayashi S, Neo M, Suzuki J, Kokubo T, Nakamura T. (2005) Mechanical properties and osteoconductivity of porous bioactive titanium. Biomaterials. 26: 6014-6023.

[33] Wen CE, Yamada Y, Shimojima K, Chino Y, Asahina T, Mabuchi M. (2002) Processing and mechanical properties of autogenous titanium implant materials. J. mat. sci. mat. med. 13: 397-401.

[34] Thelen S, Barthelat F, Brinson LC. (2004) Mechanics considerations for microporous titanium as an orthopedic implant material. J. biomed. mat. res. A. 69: 601-610.

[35] Oliveira PT, Nanci A. (2004) Nanotexturing of titanium-based surfaces upregulates expression of bone sialoprotein and osteopontin by curtured osteogenic cells. Biomaterials. 25: 403-413.

[36] Borsari V, Giavaresi G, Fini M, Torricelli P, Tschon M, Chiesa R, Chiusoli L, Salito A, Volpert A, Giardino R. (2005) Comparative in vitro study on a ultra-high roughess and dense titanium coating. Biomaterials. 26: 4948-4955.

[37] Mendonça G, Mendonça DB, Simões LG, Araújo AL, Leite ER, Duarte WR, et al. (2009) (b) Nanostructured alumina-coated implant surface: effect on osteoblast-related gene expression and bone-to-implant contact in vivo. Int. j. oral maxillofac. implants. 24: 205–215.

[38] Mendonça G, Mendonça DB, Simões LG, Araújo AL, Leite ER, Duarte WR, et al. (2009) (a) The effects of implant surface nanoscale features on osteoblastspecific gene expression. Biomaterials. 30: 4053–4062.

[39] Schwartz Z, Lohmann CH, Sisk M, Cochran DL, Sylvia VL, Simpson J, et al. (2001) (a) Local factor production by MG63 osteoblast-like cells in response to surface roughness and 1,25-(OH)2D3 is mediated via protein kinase C- and protein kinase A-dependent pathways. Biomaterials. 22: 731-741.

[40] Schwartz Z, Lohmann CH, Vocke AK, Sylvia VL, Cochran DL, Dean DD, et al. (2001) (b) Osteoblast response to titanium surface roughness and 1a,25-(OH)2D3 is mediated through the mitogen-activated protein kinase pathway. J. biomed. mater. res. 56: 417–426.

[41] Chen XB, Li YC, Du Plessis J, Hodgson PD, Wen C. (2009) Influence of calcium ion deposition on apatite-inducing ability of porous titanium for biomedical applications. Acta biomater. 5: 1808-1820.

[42] Roy M, Bandyopadhyay A, Bose S. (2011) Induction plasma sprayed nano hydroxyapatite coatings on titanium for orthopaedic and dental implants. Surf. coat. techn. 205: 2785-2792.

[43] Zaffe D. (2005) Some considerations on biomaterials and bone. Micron. 36: 583-592.

[44] Barrère F, van der Valk CM, Meijer G, Dalmeijer RA, de Groot K, Layrolle P. (2003) Osteointegration of biomimetic apatite coating applied onto dense and porous metal implants in femurs of goats. J. biomed. mat. res. B: Appl. Biomat. 67: 655-665.

[45] Machado ACP, Oliveira MV, Pereira RP, Carvalho YR, Cairo CAA. (2009) In vivo evaluation of porous titanium implants with biomimetic coating. Key eng. mat. 396-398: 179-182.

[46] Ohtsuki C, Kamitakahara M, Miyazaki T. (2007) Coating bone-like apatite onto organic substrates using solutions mimicking body fluid. J. tiss. eng. reg. med. 1: 33-38.

[47] Kasemo B, Lausmaa J. (1988) Biomaterial and implant surfaces: a surface science approach. Int. j. oral maxillofac. implant 3: 247-59.

[48] Rak ZS, Walter J. (2005) Porous titanium foil by tape casting technique. J. mat. proc. techn. 175: 755-758.

[49] Spoerke ED, Murray NG, Li H, Brinson LC, Dunand DC, Stupp SI. (2005) A bioactive titanium foam implant for bone repair. Acta biomater. 1: 523-33.

[50] Likibi F, Assad M, Coillard C, Chabot G, Rivard CH. (2005) Bone integration and apposition of porous and non porous metallic orthopaedic biomaterials. Ann. Chirur. 130: 235-41.

[51] Li JP, Li SH, Van Blitterswijk CA, De Groot K. (2006) Cancellous bone from porous Ti6Al4V by multiple coating technique. J. mat. sci. mat. med. 17: 179-85.

[52] Svehla M, Morberg P, Zicat B, Bruce W, Sonnabend D, Walsh WR. (2000) Morphometric and mechanical evaluation of titanium implant integration: comparison of five surface structures. J biomed. mat. res. 51: 15-22.

[53] Zinger O, Zhao G, Schwartz Z, Simpson J, Wieland M, Landolt D, Boyan B. (2005) Differential regulation of osteoblasts by substrate microstructural features. Biomaterials. 26:1837-47.

[54] Sepulveda P, Bressiani AH, Bressiani JC, Meseguer L, König BJ. (2002) In vivo evaluation of hydroxyapatite foams. J. biomed. mat res. 62: 587-92.

[55] Ueta MCC, Fracote CA, Henriques VAR, Graça MLA, Cairo CAA. Densification study of titanium powder compacts. Mat. sci. forum. 2005; 498-499:211-216.

[56] Deporter DA, Todescan R, Riley N. (2002) Porous-surfaced dental implants in the partially edentulous maxilla: assessment for subclinical mobility. Int. j period. rest. dent. 22: 184-192.

[57] Pilliar RM, Deporter DA, Watson PA, Todescan R. (1998) The endopore implant-enhanced osseointegration with a sintered porous-surfaced design. Oral health, 88: 61-64.

[58] Oyonarte R, Pilliar RM, Deporter D, Woodside DG. (2005) Peri-implant bone response to orthodontic loading: Part 1. A histomorphometric study of the effects of implant surface design. Am. j. orthod. dentofacial orthop. 128: 173-81.

[59] Oliveira MV, Pereira LC, Cairo CAA. (2005) Titanium powder processing with binder addition for biomedical applications. Mat. sci. forum, 498-499: 173-178.

[60] An YB, Lee WH. (2006) Synthesis of porous titanium implants by environmental-electro-discharge-sintering process. Mat. chem. phys. 95: 242-247.

[61] Deporter DA, Watson PA, Pilliar RM, Pharoah M, Smith DC, Chipman M, Locker D, Rydall A. (1996) A prospective clinical study in humans of an endosseous dental implant partially covered with a powder-sintered porous coating: 3- to 4-year results. Int. J. oral maxillofac. impl. 11: 87-95.

[62] Pilliar DA (1998) Overview of surface variability of metallic endosseous dental implants: textured and porous surface-structured designs. Impl. dent. 7: 305-312.

[63] Oliveira MV, Pereira LC, Cairo CAA. (2002) Porous structure characterization in titanium coating for surgical implants. Mat. res. 5: 269–273.

[64] Vasconcellos LM, Oliveira FN, Leite DO, Vasconcellos LGO, Prado RF, Ramos CJ, Graça ML, Cairo CAA, Carvalho YR. (2012) Novel production method of porous surface Ti samples for biomedical application. J. mat. sci. mat. med. 23: 357-364.

[65] Medeiros WS, Oliveira MV, Pereira LC, Cairo CAA, Calixto MA. (2006) Study of calcium phosphate deposition on porous titanium samples. Mat. Sci. Forum. 530-531: 569-574.

[66] Eisenbarth E, Velten D, Breme J. (2007) Biomimetic implant coatings. Biomol. eng. 24: 27-32.

[67] Rigo ECS, Boschi AO, Yoshimoto M, Allegrini JS, Konig JB, Carbonari MJ. (2004) Evaluation in vitro and in vivo of biomimetic hydroxyapatite coated on titanium dental implants. Mat sci eng C. 24: 647-651.

[68] Nishiguchi S, Nakamura T, Kobayashi M, Kim HM, Miyaji F, Kokubo T. (1999) The effect of heat treatment on bone-bonding ability of alkali-treated titanium. Biomaterials. 20: 491-500.

[69] Mamalis AA, Silvestros SS. (2011) Analysis of osteoblastic gene expression in the early human mesenchymal cell response to a chemically modified implant surface: an in vitro study. Clin. oral implants res. 22: 530-7.